Short Papers

Passive Vibration Control via Electromagnetic Shunt Damping

Sam Behrens, Andrew J. Fleming, and S. O. Reza Moheimani

***Abstract*—This paper will present a new type of passive vibration control technique based on the concept of electromagnetic shunt damping. The proposed technique is similar to piezoelectric shunt damping, as an appropriately designed impedance is shunted across the terminals of the transducer. Theoretical and experimental results are presented for a simple electromagnetic mass spring damper system.**

***Index Terms*—Control, damping, electromagnetic, shunt, vibration.**

I. Introduction

Electromagnetic transducers can be used as actuators, sensors, or both [1]–[7]. Piezoelectric transducers [7] exhibit similar electromechanical properties, but have considerably different physical and electrical characteristics to electromagnetic transducers. Electromagnetic transducers have a much greater stroke, typically in the millimeter range, compared to the micrometer range associated with piezoelectric transducers. Subsequently, in applications where piezoelectric transducers can not be used, due to their limited stroke, electromagnetic transducers may serve as a viable alternative. These devices are physically robust and can be manufactured to either MEMS scale [8] or as large as a 50-kN electrodynamic shaker [9]. Also, electromagnetic transducers are easier to drive due to their resistive-inductive nature.

Placing an electrical impedance across the terminals of a piezoelectric transducer, which is bonded to a resonant structure with the view to minimizing structural vibrations, is referred to as piezoelectric shunt damping [10]–[12]. This has been proven to be a reliable alternative to active control techniques [7], offering the benefits of stability and performance without the need of additional sensors. Most importantly, the inherent robustness makes passive shunt control techniques very desirable.

This brief presents the concept of electromagnetic shunt damping for structural vibration control. By attaching an electromagnetic transducer to a resonant mechanical structure and shunting the transducer with an electrical impedance, kinetic energy from the resonant structure can be dissipated. As the mechanical structure displaces, an opposing electro-motive-force (emf) is induced in the transducer. Using an appropriately designed electrical shunt the transducer is capable of significantly reducing mechanical vibration.

II. Background

The following sections are concerned with the modeling of an electromagnetic transducer and a simple force mass spring damper system.

Manuscript received March 12, 2003; revised September 16, 2003. This work was supported by the Australian Research Council (ARC).

The authors are with the School of Electrical Engineering and Computer Science, University of Newcastle, Callagahan 2308, Australia (e-mail: reza@ee.newcastle.edu.au).

Digital Object Identifier 10.1109/TMECH.2004.835341

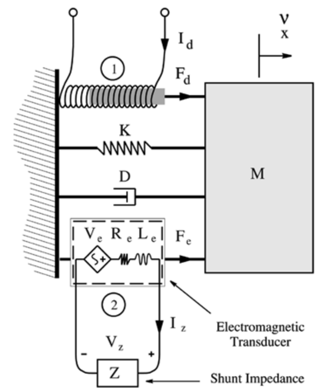

Fig. 1. Electromagnetic shunted mass spring damper system.

A. Electromagnetic Transducer Model

When an electrical conductor, in the form of a coil, moves in a magnetic field, as shown in Fig. 1, a voltage V_e proportional to the velocity ν is induced and appears across the terminals of the coil, i.e., $V_e \propto \nu$. Specifically

$$\frac{V_e}{\nu} = Bl \tag{1}$$

where B is the magnetic flux (in tesla), l is the length of the conductor (in m), and ν is the velocity of the conductor relative to the magnetic field (in m/s). A permanent magnet is usually the source of the magnetic field.

Assuming the coil is exposed to a field of constant flux density and the relative displacement is small, (1) can be rewritten as [13]

$$\frac{V_e}{\nu} = \frac{F_e}{I_z} = Bl = C_e \tag{2}$$

where F_e denotes the force (in N) acting on the coil while carrying a current I_z (in A), and C_e is the ideal electro-mechanical coupling coefficient (in N/A or V/m·s^{-1}).

When a coil is employed as a force actuator, (2) relates the induced force to an applied current. Such designs form the basis for electrodynamic shakers and acoustic actuators, such as a speaker coils. As shown in Fig. 1, the coil can be modeled as series connection of an inductor L_e, a resistor R_e, and a dependent voltage source V_e [2]. If the transducer is attached to a resonant mechanical system, the voltage source V_e, represents the induced emf that is dependent on relative velocity ν, and hence, structural dynamics.

B. Forced Mass Spring Damper System

In many cases where vibration becomes an issue, the mechanical structure can be modeled as a simple mass spring damper system. The equivalent mass M (in kg), spring constant K (in N/m) and damping constant D (in N·s/m) for such a structure can be easily determined. The equation of motion for this forced one degree of freedom (DOF) system is given by

$$M\ddot{x}(t) + D\dot{x}(t) + Kx(t) = F_d(t), \tag{3}$$

where $\ddot{x}(t)$, $\nu(t)$, and $x(t)$ are the acceleration, velocity, and displacement of the mass, respectively. Note that $F_d(t)$ is the applied force disturbance. The dimensionless representation of (3) is

$$\ddot{x}(t) + 2\zeta_n \omega_n \dot{x}(t) + \omega_n^2 x(t) = f_d(t) \tag{4}$$

where ω_n is the natural frequency of the system, and ζ is the damping ratio. Note that $\omega_n = \sqrt{(K/M)}, \zeta_n = (D/\sqrt{4MK})$ and $f_d(t) = (F_d(t))/(M)$.

III. Structural Dynamics From First Principles

Electromagnetic shunt damping is modeled for a simple electromagnetic mass spring damper system. The composite system will be derived from fundamental principles.

A. Model System

Consider Fig. 1, where an electromagnetic transducer (coil 1) is attached to a mass M. If a current $I_d(t)$ is applied to a linear electromagnetic transducer, a disturbance force $F_d(t)$ is induced such that $F_d(t) = C_d I_d(t)$, where C_d is the electromagnetic coupling coefficient relating the applied current to a resulting force in coil 1. Using the equation of motion, the disturbed system has the following relationship, $M\ddot{x}(t) + D\dot{x}(t) + Kx(t) = C_d I_d(t)$.

By taking the Laplace transform, the transfer functions relating the current $I_d(s)$ to displacement $x(s)$ is found to be

$$G_{\mathrm{xi}}(s) \triangleq \frac{x(s)}{I_d(s)} = \frac{C_d}{\mathrm{Ms}^2 + \mathrm{Ds} + K}, \tag{5}$$

and the current $I_d(s)$ to velocity $\nu(s)$ is

$$G_{\nu i}(s) \triangleq \frac{\nu(s)}{I_d(s)} = \frac{C_d s}{Ms^2 + Ds + K}. \tag{6}$$

These equations are valid when coil 2 is held in open circuit, i.e., $Z(s) = \infty$, as shown in Fig. 1. Note that velocity $\nu(s)$ is equivalant to $\mathrm{sx}(s)$ in the Laplace domain.

B. Composite System

For an electromagnetic shunted composite system, as shown in Fig. 1, an impedance Z is attached to coil 2. We have the following relationship, $M\ddot{x}(t) + D\dot{x}(t) + \mathrm{Kx}(t) = F_d(t) - F_e(t)$, where $F_e(t)$ is the opposing force due to the impedance Z attached to the terminals of the electromagnetic transducer. In the Laplace domain, we have the following relationship:

$$x(s)(\mathrm{Ms}^2 + \mathrm{Ds} + K) = C_d I_d(s) - F_e(s) \tag{7}$$

where $I_d(s)$ is the input current applied to coil 1, as shown in Section III-A.

To determine the opposing force $F_e(s)$, we need to consider the simplified electrical model of the electromagnetic shunt, as shown in Fig. 1. Ohm's law states that

$$V_z(s) = I_z(s) Z(s) \tag{8}$$

where $V_z(s)$ is the voltage across the terminals of the shunt impedance $Z(s)$, and $I_z(s)$ is the corresponding current. According to Kirchhoff's voltage law, we obtain the following relationship between $V_e(s)$ and $V_z(s)$, as $V_z(s) = V_e(s) - (L_e s + R_e) I_z(s)$, which implies

$$V_z(s) = \frac{Z(s)}{Z(s) + L_e s + R_e} V_e(s). \tag{9}$$

As shown in (1), we have the following linear relationship:

$$V_e(s) = C_e \nu(s) \tag{10}$$

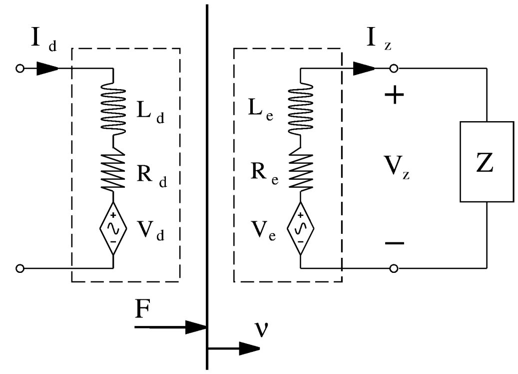

Fig. 2. Electrical equivalent model of a twin-coil electromagnetic system.

where C_e is the electromagnetic constant relating $\nu(s)$ to $V_e(s)$ of coil 2.

By substituting, (10) into (9), we obtain

$$V_z(s) = \frac{Z(s)}{Z(s) + L_e s + R_e} C_e \nu(s). \tag{11}$$

Alternatively, the current flowing through the shunt $I_z(s)$ is

$$I_z(s) = \frac{V_z(s)}{Z(s)} = \frac{1}{Z(s) + L_e s + R_e} C_e \nu(s) \tag{12}$$

and the opposing shunt force $F_e(s) = C_e I_z(s)$, assuming a linear electromagnetic transducer, we obtain

$$F_e(s) = \frac{C_e^2}{L_e s + R_e + Z(s)} \nu(s) = C_e^2 \hat{K}(s) \nu(s) \tag{13}$$

where $\hat{K}(s) = (1)/(L_e s + R_e + Z(s))$.

Substituting (13) into (7), the composite system transfer function $I_d(s)$ to $x(s)$ can be obtained

$$\hat{G}_{\mathrm{xi}}(s) \triangleq \frac{x(s)}{I_d(s)} = \frac{C_d}{Ms^2 + \left(D + C_e^2 \hat{K}(s)\right) s + K}. \tag{14}$$

Alternatively, the transfer function relating $I_d(s)$ to $\nu(s)$ is

$$\hat{G}_{\nu i}(s) \triangleq \frac{\nu(s)}{I_d(s)} = \frac{C_d s}{Ms^2 + \left(D + C_e^2 \hat{K}(s)\right) s + K}. \tag{15}$$

IV. Composite System in Transfer Function Form

By modeling the system in transfer function form, we gain a greater abstraction from the underlying system. Such methods are particularly useful when dealing with higher order systems or when using models not obtained directly through physical modeling, i.e., when using models obtained by means of system identification [14]. Referring to Fig. 2, the models required are $G_{\nu F}(s)$, the transfer function from an applied force to the resulting velocity ν; and $G_{\mathrm{vi}}(s)$ is the the transfer function from an applied current to the induced emf.

We first consider the case where two identical coils experience the same velocity. When an impedance $Z(s)$ is attached to coil 2, $V_z(s) = V_e(s) - (L_e s + R_e) I_z(s)$. That is

$$V_z(s) = \frac{Z(s)}{L_e s + R_e + Z(s)} V_e(s) \tag{16}$$

$$I_z(s) = \frac{1}{L_e s + R_e + Z(s)} V_e(s). \tag{17}$$

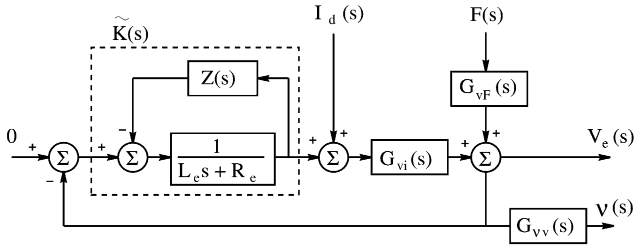

Fig. 3. Regulator feedback structure associated with the electromagnetic shunt damping.

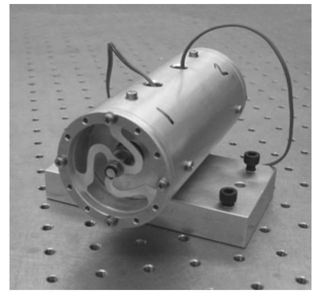

Fig. 4. External photograph of the experimental electromagnetic apparatus.

By considering the emf induced in both coils 1 and 2 and applying the principle of superposition, $V_e(s) = G_{\rm vi}(s)I_d(s) - G_{\rm vi}(s)I_z(s)$. Substitution of (17) yields $V_e(s) = G_{\rm vi}(s)I_d(s) - G_{\rm vi}(s)(V_e(s))/(L_e s + R_e + Z(s))$. Hence, the composite transfer function relating $I_d(s)$ to $V_e(s)$ is

$$\tilde{G}_{\rm vi}(s) \triangleq \frac{V_e(s)}{I_d(s)} = \frac{G_{\rm vi}(s)}{1 + \tilde{K}(s)G_{\rm vi}(s)} \tag{18}$$

where $\tilde{K}(s) = (1)/(L_e s + R_e + Z(s))$. The reader will appreciate that the damped system transfer function $\tilde{G}_{\rm vi}(s)$ is in the form of a feedback system where the impedance $Z(s)$ parameterizes a controller $\tilde{K}(s)$, as shown in Fig. 3.

This is an interesting observation as it enables one to employ systems theoretic tools to analyze the dynamics of the shunted system. The feedback control problem associated with (18) is illustrated in Fig. 3. The reader can observe that the purpose of the control system is to regulate $V_e(s)$, or alternatively $\nu(s)$, in the presence of a disturbance $I_d(s)$, as shown in Fig. 3.

In a more general case, we wish to know the damped transfer function $\tilde{G}_{\nu F}(s)$ from some disturbance force $F(s)$ to the resulting velocity $\nu(s)$. Noting that the undamped transfer function $G_{vi}(s)$ consists of both the structural dynamics and the electromagnetic coupling $G_{vi}(s) = C_e G_{\nu i}(s) = C_e^2 G_{\nu F}(s)$, this is easily found to be

$$\begin{aligned} \tilde{G}_{\nu i}(s) &\triangleq \frac{\nu(s)}{I_d(s)} \\ &= \frac{V_e(s)}{I_d(s)}\frac{\nu(s)}{V_e(s)} \\ &= \tilde{G}_{\rm vi}(s)\frac{\nu(s)}{V_e(s)} \\ &= \frac{G_{\nu i}(s)}{1 + \tilde{K}(s)G_{\rm vi}(s)}. \end{aligned} \tag{19}$$

Thus, $\tilde{G}_{\nu F}(s) \triangleq (\nu(s)/F(s)) = (\nu(s))/(C_e I_d(s)) = (1)/(C_e)\tilde{G}_{\nu i}(s)$, and

$$\nu(s) = \frac{G_{\nu i}(s)}{1 + \tilde{K}(s)G_{\rm vi}(s)}I_d(s) + \frac{G_{\nu F}(s)}{1 + \tilde{K}(s)G_{\rm vi}(s)}F(s) \tag{20}$$

as shown in Fig. 3.

V. Single Mode Electromagnetic Shunt Controller

Hagood and von Flotow [11] suggested that a series of resistor-inductor circuit attached across the conducting surfaces of a piezoelectric transducer can be tuned to dissipate the mechanical energy of a host structure. They demonstrated the effectiveness of this technique by tuning the resulting resistor–inductor (R–L) circuit and inherent capacitance of the piezoelectric transducer, to a specific resonance frequency of the host structure.

For electromagnetic shunt damping, we can apply the same methodology as suggested above. For this particular system, though, we need to apply a resistor–capacitor (R–C) circuit to the terminals of the electromagnetic transducer. That is, $Z(s) = (1)/(Cs) + R$, where the capacitance value is determined by $\omega_n^2 = (1)/(\mathrm{C}L_e)$, L_e denotes the inherent inductance of the electromagnetic transducer to be shunted, and ω_n is the resonance frequency of the mechanical structure to be controlled. For example, for a simple mass spring damper system as shown in Fig. 1, the capacitance is $C = (1)/(\omega_n^2 L_e) = (1)/((K/M)L_e)$, where K is the spring constant and M the mass of the mechanical system.

The shunted electromagnetic transducer, $\nu(s)$ is related to F_e via $F_e(s) = C_e^2 K_p(s)\nu(s)$, where $K_p(s) = ((1/L_e))/(s^2 + (R_t/L_e)s + (1/\mathrm{C}L_e))$. It should be noted that the controller has a resonant structure; thus, $R_t = (R_e + R)$ determines the controller damping. To determine the optimal total resistance R_t, an optimization strategy could be used. For a more detailed explanation for the optimization strategy the reader is referred to Behrens *et al.* [15].

The damped composite transfer function from disturbance current I_d, to velocity ν, is $\hat{G}_{\nu i}(s) \triangleq (\nu(s))/(I_d(s)) = (C_d s)/(\mathrm{M}s^2 + (D + C_e^2 K_p(s))s + K)$ or, alternatively, $\tilde{G}_{\nu i}(s) \triangleq (\nu(s))/(I_d(s)) = (G_{\nu i}(s))/(1 + K_p(s)G_{\rm vi}(s))$.

VI. Experimental Verification of Electromagnetic Shunt Damping Concept

In this section, we will consider the electromagnetic experimental apparatus, a method for determining the optimal shunt resistance and a technique for synthesizing the required shunt impedance. Comparison between theoretical and experimental results is also presented.

A. Electromagnetic Apparatus

In support of the preceeding sections, the technique of electromagnetic shunt damping was applied to an experimental assembly at the Laboratory for Dynamics and Control of Smart Structures, The University of Newcastle, Australia.[1] A photograph of the electromagnetic transducer apparatus, showing the rigid external support, flexible end supports, mounting plate, coils, and winding cables is provided in Fig. 4. As shown in Fig. 5, the assembly is essentially a translational solenoid with two identical fixed coils and a magnetic plunger supported at either end by flexible supports. This system is mechanically equivalent to the mass spring damper shown in Fig. 1. Together with an attached electrical impedance $Z(s) = (1/Cs) + R$, coil 2 is employed to damp translational vibrations resulting from an applied disturbance current I_d to coil 1. For a detailed description of

[1]http://rumi.newcastle.edu.au/lab

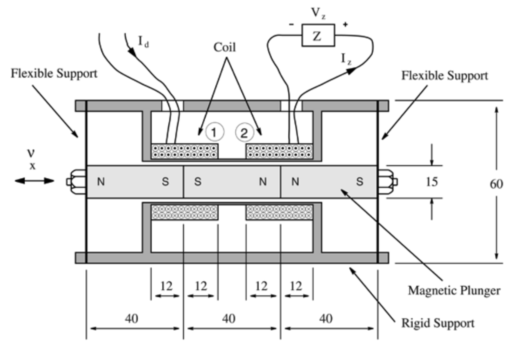

Fig. 5. Side section of the experimental electromagnetic apparatus (all dimensions in millimeters).

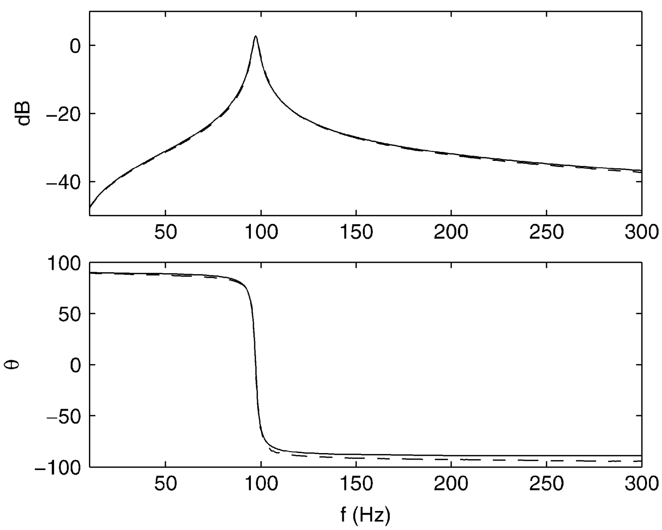

Fig. 6. Undamped frequency response from an applied actuator current to plunger velocity, i.e., $G_{\nu i}(s)$, model (–) and measured results (- -).

the electromagnetic apparatus, the reader is referred to Behrens *et al.* [15].

B. Determining Optimal Damping Resistance

The electromechanical model $G_{\nu i}(s)$ was first determined by measuring the resonance frequency and plunger weight M and, subsequently, the spring constant K. The remaining parameter ω_n, together with the electromagnetic coupling coefficients C_d and C_e, were determined experimentally. Experimental apparatus parameters are $M = 0.15$ Kg, $D = 2.677$ Nsm^{-1}, $K = 56$ kNm^{-1}, $C_e = 3.4$ N/A or V/ms^{-1}, $C_d = 3.65$ N/A, $L_e = 1$ mH, and $R_e = 3.3\ \Omega$. The frequency response from an applied current to the resulting plunger velocity $G_{\nu i}(s)$ is shown in Fig. 6. It is observed that the model is an accurate representation of the physical system.

Since we wish to damp the fundamental frequency of the mass spring damper system, i.e., $\omega_n = 2\pi\sqrt{(K/M)} = 97.3$ Hz, the required shunt capacitance value is $C = (1)/(\omega_n^2 L_e) = (1)/((K/M)L_e) = 2.7$ mF.

In order to determine an appropriate value for the total shunt resistance R_t, an optimization approach was used to minimize the $\mathcal{H}_2$ norm of the damped system $\hat{G}_{\nu i}(s)$ [15]. This required a solution to the following optimization problem to be found $R_t^* = \arg\min \|\hat{G}_{\nu i}(s)\|_2$ for $R_t > 0$. Using the proposed optimization strategy the required optimal shunt resistance is found to be $R_t^* = 0.29\ \Omega$.

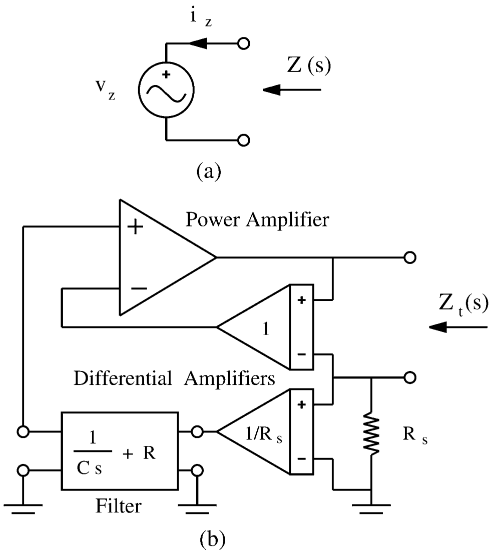

Fig. 7. (a) Ideal current controlled voltage source. (b) Experimental current controlled voltage source.

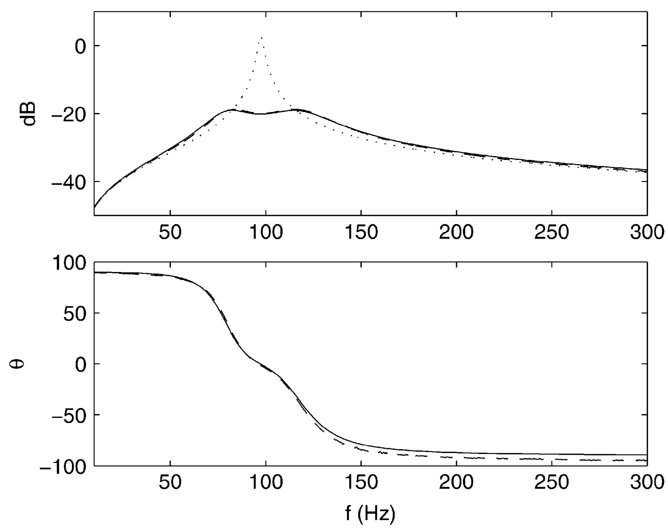

Fig. 8. Undamped $(\cdots)$, theoretically predicted damped (–), and measured damped (- -) frequency responses from an applied current to the resulting plunger velocity $\hat{G}_{\nu i}(s)$.

C. Impedance Implementation

To implement the proposed arbitrary shunt impedance $Z(s)$, a current controlled voltage source was utilized, as shown in Fig. 7. The controlled voltage v_z was set to be a function of the measured current i_z, i.e., $v_z(t) = f(i_z(t))$, as shown in Fig. 7(a). If the function $f(i_z(t))$, is a linear transfer function $Z(s)$ whose input impedance is the measured current $I_z(s)$, i.e., $V_z(s) = Z(s)I_z(s)$, then the terminal impedance $Z_t(s)$ is equal to $Z(s)$, as shown in Fig. 7(b). For a more detailed description of the impedance apparatus, the reader is referred to Fleming *et al.* [16], [17].

D. Simulated versus Experimental Results

With the aim of damping the system, a total series resistance $(R_e + R)$ of 0.35 Ω and a capacitance 2.7 mF were tuned online to the second winding using the synthetic impedance apparatus explained in Section VI-C. The measured undamped, theoretically predicted damped, and measured damped frequency responses are shown in Fig. 8. A significant reduction of 21.8 dB in the magnitude of the electromechanical system is observed. An inconsistency between the theoretical and experimental resistance R_t^* was noted and can be attributed to the tolerance of sensing resistance R_s in the synthetic impedance apparatus, as shown in Fig. 7. Overall, simulated and experimental results closely agree, therefore, validating the proposed electromagnetic shunt damping technique.

VII. Conclusion

In this brief, we have introduced a new type of vibration control method based on the concept of electromagnetic shunt damping. The proposed technique was experimentally validated on a simple electromagnetic mass spring damper system. A 21.8-dB peak amplitude reduction was achieved via simulation and experimentation.

References

[1] S. Mirzaei, S. M. Saghaiannejad, V. Tahani, and M. Moallem, "Linear electric actuators and generators," *IEEE Trans. Energy Convers.*, vol. 14, pp. 712–717, Sept. 1999.

[2] B. M. Hanson, M. D. Brown, and J. Fisher, "Self sensing: Closed-loop estimation for a linear electromagnetic actuator," in *Proc. IEEE American Control Conf.*, Arlington, VA, June 2001, pp. 1650–1655.

[3] Y. B. Kim, W. G. Hwang, C. D. Kee, and H. B. Yi, "Active vibration control of suspension system using an electromagnetic damper," in *Proc. Int. MECH Eng. Part D J. Automoblie Eng.*, vol. 8, 2001, pp. 865–873.

[4] J. Shaw, "Active vibration isolation by adaptive control," in *Proc. IEEE Int. Conf. Control Applications*, Aug. 1999, pp. 1509–1514.

[5] D. Vischer and H. Bleuler, "Self-sensing active magnetic levitation," *IEEE Trans. Magn.*, vol. 29, pp. 169–177, Feb. 1993.

[6] N. Morse, R. Smith, B. Paden, and J. Antaki, "Position sensed and self-sensing magnetic bearing configuations and associated robustness limitations," in *Proc. IEEE Conf. Decision Control*, Tampa, FL, Dec. 1998, pp. 2599–2604.

[7] C. R. Fuller, S. J. Elliott, and P. A. Nelson, *Active Control of Vibration*, New York: Academic, 1996.

[8] R. Amirtharajah and A. P. Chandrakasan, "Self-powered signal processing using vibration-based power generation," *IEEE J. Solid-State Circuits*, vol. 33, pp. 687–695, May 1998.

[9] Large Shaker Model V53-64/DSA4 [Online]. Available: http://www.gearing-watson.com

[10] R. L. Forward, "Electronic damping of vibrations in optical structures," *Appl. Opt.*, vol. 18, no. 5, pp. 690–697, Mar. 1979.

[11] N. W. Hagood and A. Von Flotow, "Damping of structural vibrations with piezoelectric materials and passive electrical networks," *J. Sound Vibration*, vol. 146, no. 2, pp. 243–268, 1991.

[12] S. Behrens, S. O. R. Moheimani, and A. J. Fleming, "Multiple mode current flowing passive piezoelectric shunt controller," *J. Sound Vibration*, vol. 266, no. 5, pp. 929–942, Oct. 2003.

[13] S. S. Rao, *Mechanical Vibrations*, 3rd ed. Reading, MA: Addison-Wesley, 1995.

[14] L. Ljung, *System Identification: Theory for the User*. Englewood Cliffs, NJ: Prentice-Hall, 1999.

[15] S. Behrens, A. Fleming, and S. O. R. Moheimani, "Electromagnetic shunt damping," in *Proc. IEEE Int. Conf. Advanced Intelligent Mechatronics 2003*, Kobe, Japan, July 2003.

[16] A. J. Fleming, S. Behrens, and S. O. R. Moheimani, "Synthetic impedance for implementation of piezoelectric shunt-damping circuits," *Electron. Lett.*, vol. 36, no. 18, pp. 1525–1526, Aug. 2000.

[17] A. Fleming and S. O. R. Moheimani, "Precision current and charge amplifiers for driving highly capacitive piezoelectric loads," *Electron. Lett.*, vol. 39, no. 3, pp. 282–294, Feb. 2003.

Disturbance Modeling and Control Design for Self-Servo Track Writing

Chunling Du, Jingliang Zhang, and Guoxiao Guo

***Abstract*—In this paper, the major disturbances in self-servo track writing are identified and modeled. Based on the disturbance models, an H_2 controller together with a feedforward compensator is designed via linear matrix inequality approach to minimize the propagation tracking error from one track to the next. Furthermore, the error propagation containment effectiveness of the optimal H_2 control is compared with that of proportional–integral–derivative (PID) and proportional-derivative (PD) feedback controls with the feedforward compensators. Our results show that the propagation tracking error is improved by 27% with the H_2 control compared with that by PID control.**

***Index Terms*—Linear matrix inequality, optimal control, servo track writing, self-servo track writing.**

Nomenclature

HDD	Hard disk drive.
VCM	Voice-coil motor.
GMR	Giant magnetoresistive.
STW	Servo track writing.
SSTW	Self-servo track writing.
R/W	Read/write.
TPI	Track per inch.
TMR	Track mis-registration.
PES	Position error signal.
RRO	Repeatable runout.
NRRO	Nonrepeatable runout.
LMI	Linear matrix inequality.

I. Introduction

Increased storage capacity in HDDs is directly attributed to the high-track density achievable with servo positioners and the GMR head technology that allow reading and writing narrower tracks. As technology advances to provide smaller disk drives and increased track densities, the accurate placement of servo information (or "servo bursts") must also increase proportionately. Servo bursts are conventionally written by costly dedicated servowriting equipment external to the disk drive with a laser-guided mechanism to position write head on the desired disk surface. With the increase of track density to above 100 000 TPI, the disk and motor vibrating in nanometer scale makes the accurate control of R/W head alone in the STW process insufficient. Self-servo track writing has been developed as an approach to support ultrahigh TPI at a low cost [2], [5], [12].

In the SSTW, track shape errors introduced by mechanical disturbances are mainly due to disk and motor. Such errors may be reproduced from one track to the next because the servo controller causes the actuator to follow the previously written track when writing the next track patterns. As a result, each step in the process carries a memory of all preceding track shape errors, which is called error propagation [2], [13]. SSTW systems need to correct the error propagation by using controllers. One measure of the control performance is TMR [1], the total amount of random fluctuation of the R/W head off the desired track

Manuscript received September 12, 2002; revised September 3, 2003, December 8, 2003, February 16, 2004.

The authors are with A*STAR, Data Storage Institute (DSI), Kent Ridge Crescent, NUS, Singapore (e-mail: DU_Chunling@dsi.a-star.edu.sg).

Digital Object Identifier 10.1109/TMECH.2004.835343